Shear viscosity for dense plasmas by equilibrium molecular dynamics in asymmetric Yukawa ionic mixtures

Tomorr Haxhimali, Robert E. Rudd, William H. Cabot, and Frank R. Graziani

Shear viscosity for dense plasmas by equilibrium molecular dynamics in asymmetric Yukawa ionic mixtures

Tomorr Haxhimali,* Robert E. Rudd, William H. Cabot, and Frank R. Graziani

Lawrence Livermore National Laboratory,
Livermore, California 94550, USA

We present molecular dynamics (MD) calculations of shear viscosity for asymmetric mixed plasma for thermodynamic conditions relevant to astrophysical and Inertial Confinement Fusion plasmas. Specifically, we consider mixtures of deuterium and argon at temperatures of 100-500 eV and a number density of 10^{25} ions/cc. The motion of 30000-120000 ions is simulated in which the ions interact via the Yukawa (screened Coulomb) potential. The electric field of the electrons is included in this effective interaction; the electrons are not simulated explicitly. Shear viscosity is calculated using the Green-Kubo approach with an integral of the shear stress autocorrelation function, a quantity calculated in the equilibrium MD simulations. We systematically study different mixtures through a series of simulations with increasing fraction of the minority high-Z element (Ar) in the D-Ar plasma mixture. In the more weakly coupled plasmas, at 500 eV and low Ar fractions, results from MD compare very well with Chapman-Enskog kinetic results. In the more strongly coupled plasmas, the kinetic theory does not agree well with the MD results. We develop a simple model that interpolates between classical kinetic theories at weak coupling and the Murillo Yukawa viscosity model at higher coupling. This hybrid kinetics-MD viscosity model agrees well with the MD results over the conditions simulated, ranging from moderately weakly coupled to moderately strongly coupled asymmetric plasma mixtures.

PACS numbers: 52.25.Fi,52.27.Gr,52.29.Hq

I. INTRODUCTION

Plasma transport theory has been key to understanding a broad range of phenomena from stellar and planetary interiors [1–3] to dusty plasmas [4] to inertial confinement fusion [5]. It was formulated as an extension of the kinetic theory of gases by Chapman and Cowling [6] and subsequent authors like Spitzer [7]. While successful for weakly coupled plasmas, it is limited by its reliance on a small-angle, binary collision operator. The resulting equations for viscosity and other transport coefficients are not accurate for dense and strongly coupled plasmas [8–10]. This inaccuracy can matter for applications of current interest. For example, a recent study investigated the effect of viscosity on turbulence near the hot spot that can affect the yield in inertial confinement fusion [11, 12]. At the time of peak fuel kinetic energy [11], we find that the actual viscosity differed by as much as 70% from what the Chapman-Cowling theory [6] predicts.

Often the issue is described as an error in the Coulomb logarithm that enters the expression for the scattering integral, the logarithm of the ratio of a long-distance cutoff to a short-distance cutoff. Both of these cutoffs are somewhat ill defined for the Coulomb interaction, related respectively to the screening length and a short-distance scale such as the classical turning point or the de Broglie wavelength.

Even the case of single-species plasma is challenging, and the case of mixtures is more so. Mixtures exhibit a more diverse set of phenomena. The case of asymmetric plasmas is particularly interesting, that is mixtures in which the ionization states of the constituents differ significantly. Kinetic theory breaks down as one species in the plasma becomes strongly coupled. For example, both the syrup-like viscosity of strongly coupled dusty plasmas [13] and the vanishing viscosity of the superfluid component of Bose-Einstein condensates [14] are related to correlations that are not accounted for in conventional kinetic theory.

The viscosity of plasma mixtures is of interest for a variety of applications. Viscosity is a resistance to shear flow in the plasma. It contributes to the hydrodynamic equations that describe the plasma flow. Viscosity affects convective flow in gas giant planets and the associated convective heat losses.

And, viscosity η enters into the Reynolds number, $Re = \rho v L/\eta$, which characterizes fluid flow and the level of turbulence [15]. Here ρ is the mass density, v is a characteristic flow velocity and L is a characteristic length.

Plasma viscosity increases in both the high and low temperature limits [16, 17]. At low temperatures as the temperature is lowered further, the plasma coupling increases and correlations become more important. Eventually, the plasma undergoes a phase transformation to a solid which has strength, but even prior to that the viscosity increases as more shear stress is needed to overcome the ion-ion interactions and get the fluid to flow. Ionic correlations are very important in this regime. At high temperatures, further increasing the temperature increases the viscosity due to kinetic contribution to viscosity. The ionic potential contribution is negligible in this weakly coupled regime, but both the magnitude of

the shear stress fluctuations and the mean free time are increasing with temperature causing the viscosity to rise. That behavior from strong coupling to weak coupling has been studied extensively for single species plasmas. It is expected to apply to mixed plasmas as well, but the details are not well understood. The case of asymmetric plasma mixtures is particularly interesting. While new techniques are coming on line to measure the viscosity of plasmas such as using the Brillouin peak in x-ray Thomson scattering [18], few experimental data are available.

Here we use classical molecular dynamics (MD) to simulate the momentum transfer processes associated with the viscosity of an asymmetric plasma mixture. MD simulates the motion of ions by integrating Newton's Law (F=ma) for a large collection of ions interacting via a specified force law. MD has been shown to provide accurate values for the viscosity of strongly coupled plasmas like liquid metals [19, 20] and weakly coupled plasmas [21]. The accuracy of the predictions depends on the fidelity of the inter-ionic potential that is used, i.e., the potential from which the force law is derived. Here we use the Yukawa (screened Coulomb) potential.

The literature on computing viscosity for one component plasmas using MD is very rich. For Yukawa systems Sanbonmatsu and Murillo [22] as well as Donkó and Hartmann [23] used nonequilibrium MD (NEMD) simulations that mimic experiment by applying an external shear. On the other hand viscosity can be extracted by equilibrium MD (EMD) in the limit of very small stress. In equilibrium conditions the momentum transport arises from gradient in velocity, created from thermal fluctuations, without any imposed shear. Using equilibrium MD Bastea [24] computed the shear viscosity for one component plasmas immersed at a rigid neutralizing electron background for coupling that ranges from 0.05 to 100. Recently the work of Daligault et al. [21] has extended the study of viscosity to couplings as low as 0.01 and built a model that reproduces the Landau-Spitzer form at weakly coupled limit and compares well with the Bastea results at moderate and strongly coupled limit. A thorough parametric study of viscosity for one component Yukawa systems was conducted by Saigo and Hamaguchi [17] and Salin and Caillol [25]. Donkó et al. have used both EMD and NEMD to study viscoelstic response of strongly coupled Yukawa liquids [26]. An extension of the Chapman-Cowling method to compute transport coefficients including viscosity, to the strongly coupled limit for one component Yukawa systems has been recently introduced and tested with MD [27].

For Yukawa binary mixtures a parametric study of shear viscosity and thermal conductivity was conducted by Salin and Gilles [28]. They limited this study to mixtures where the mass ratio of the ion species was assumed the same with the charge ratio and kept at a constant value 5. Bastea [24] developed a model for the viscosity of binary mixtures that was derived by using effective medium theory. To include the effect of the electrons, Murillo [19] proposed a quasiuniversal viscosity model

for Yukawa systems. To extend his model to mixtures he suggested to use the effective Coulomb coupling Γ_{eff}.

Despite this body of work, important questions remain unresolved: For what range of thermodynamic conditions classical kinetic description of viscosity, like Landau-Spitzer and Chapman-Enskog, remain valid in asymmetric mixed plasmas? What is the effect of a strongly correlated component in the nature of momentum transport? How accurate are the existing mixing rules? We address these questions here.

The article is organized as follows. In Section II a description of the condition of mixed plasmas studied is followed by a short review of the Green-Kubo technique used to extract shear viscosity, and details of the MD simulations. In Section III, MD results are shown. In Section IV we compare our MD results of shear viscosity with those from kinetic theories. Existing mixing rules are tested with respect to MD and a new mixing rule is introduced in Section V. Summary is finally given in Section VI.

II. FORMULATION AND METHODOLOGY

A. Mixed plasma description

In this work we focus on plasma consisting of binary mixtures of deuterium and argon ions at dense conditions with a total number density of $n = 10^{25}$ ions/cc and temperatures T from 100 to 500 eV. At these conditions it is a good approximation to treat the ions as statically screened electric charges by a polarizable free electron background. The electrons adiabatically follow ionic dynamic, and as a result the ions will interact with each other through an effective screened Coulomb interaction potential. Within linear response theories [29, 30] the interaction between ions is the Yukawa potential [31]:

$$V(\mathbf{r}_{ij}) = \frac{Z_i^* Z_j^* e^2}{4\pi\epsilon_0 r_{ij}} \exp(-r_{ij} k_{D,e}), \qquad (1)$$

where Z_i^* and Z_j^* are the average ionized charges of ions i and j and $\mathbf{r}_{ij}$ is their distance. This potential captures the electron polarizability in a linear response regime [29, 30]. Several recent articles [32–34] have verified its validity in warm and hot dense matter regimes, and it is expected to provide an accurate description of the 100 eV and hotter plasmas studied here. Polarizable BIM models [35–37] have been developed for binary mixed plasmas based on a similar motivation. In the linear response limit the screening coefficient due to the electrons $k_{D,e}$ that enters in the Yukawa potential (1) may be approximated as [19, 38, 39]:

$$k_{D,e} \approx \sqrt{\frac{n_e e^2}{\epsilon_0 \sqrt{(k_B T)^2 + \left(\frac{2}{3} E_F\right)^2}}}. \qquad (2)$$

This expression for the screening coefficient is a Debye-Hückel [40] form with an effective temperature that accounts for the partial degeneracy of the electrons using the Fermi energy of the free electron gas

$$E_F = \hbar^2 (3\pi^2 n_e)^{2/3} / 2m_e. \tag{3}$$

Here m_e is the electron mass. Due to global charge neutrality, the electron density n_e is related to ion density and the average charge $\langle Z^* \rangle$ of the mixture by $n_e = \langle Z^* \rangle n$. Unless otherwise mentioned in this article the angular brackets $\langle \cdots \rangle$ represent a mole fraction weighted average of thermodynamical variable Ξ, such that $\langle \Xi \rangle \equiv \sum_i X_i \Xi_i$, where X_i is the mole fraction of species i.

Yukawa (screened Coulomb) systems can be described by two dimensionless parameters, eliminating the dimensions of length using the Wigner-Seitz radius, $r_{ws} = \left(\frac{3}{4\pi n} \right)^{1/3}$. The two dimensionless parameters are the screening coefficient $\kappa = r_{ws} k_{D,e}$ [4] and the Coulomb coupling coefficient $\Gamma = (Z^*)^2 e^2 / 4\pi \epsilon_0 r_{ws} k_B T$, which is the ratio of the average Coulomb energy to the thermal kinetic energy. These are the only two dimensionless parameters of a single-species Yukawa system. Alternatively, one can use the coupling strength which is the ratio of the average nearest neighbors interionic potential to the kinetic energy. For Yukawa systems this is approximately given by $e^{-\kappa} \Gamma$. An accurate definition and computation of the coupling strength for Yukawa systems can be found in the work by Ott et al. [41].

The Coulomb coupling of the mixtures is usually described as an average over the coupling of each species:

$$\Gamma_{\text{eff}} = X_1 \Gamma_1 + X_2 \Gamma_2, \tag{4}$$

where $\Gamma_i = (Z_i^*)^2 e^2 / 4\pi \epsilon_0 r_i k_B T$ is the coupling of the component i in the mixture. The "ion-sphere" radius [42, 43] r_i given by

$$r_i \equiv \left(\frac{3}{4\pi n_e} Z_i^* \right)^{1/3} = \left(\frac{3}{4\pi n} \frac{Z_i^*}{\langle Z^* \rangle} \right)^{1/3} = r_{ws} \left(\frac{Z_i^*}{\langle Z^* \rangle} \right)^{1/3}, \tag{5}$$

represents a neutral sphere, where the charge of the free electrons compensates for the charge of the ions. This compensation reflects the local charge neutrality. Using Eq. (5) gives the following expression for Γ_i:

$$\Gamma_i = \frac{1}{4\pi\epsilon_0} \frac{\langle Z \rangle^{1/3} Z_i^{5/3} e^2}{k_B T r_{ws}}. \tag{6}$$

Plugging Eq. (6) into Eq. (4) gives the following for the effective Coulomb coupling of a binary mixture:

$$\Gamma_{\text{eff}} = \frac{\langle Z^* \rangle^{1/3} \langle (Z^*)^{5/3} \rangle e^2}{4\pi\epsilon_0 r_{ws} k_B T}. \tag{7}$$

Alternatively the effective coupling for Yukawa binary mixture considering the dimensionless screening is approximately given by $e^{-\kappa} \Gamma_{\text{eff}}$. For the conditions that

we studied here the dimensionless screening κ varied in the range $\kappa \in [0.57, 1.57]$ and the Coulomb effective coupling $\Gamma_{\text{eff}} \in [0.88, 34.85]$.
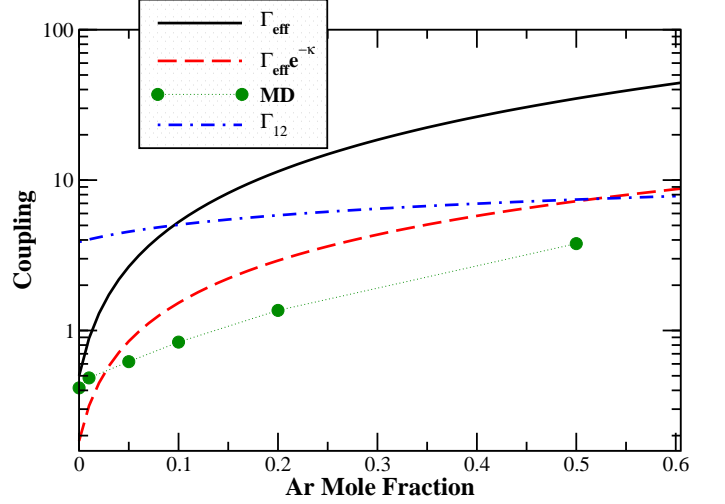

FIG. 1. (Color online) Effective coupling for D-Ar mixture at 100 eV and ion density 10^{25} cm^{-3} as a function of Ar mole fraction. The ionized charges of the two species are kept constant at $Z_{\text{Ar}}^* = 13$ and $Z_{\text{D}}^* = 1$. With black solid line we plot the value of the Coulomb effective coupling Γ_{eff} from Eq. (7). The red dashed line represents values of the Yukawa coupling $e^{-\kappa} \Gamma_{\text{eff}}$, and the blue dashed-dot line corresponds to values computed for Γ_{12} in Eq. (8). In the same figure we show the system coupling as measured directly from MD.

Another form found in literature [38, 44] that describes the coupling of the binary mixture is:

$$\Gamma_{12} = \frac{Z_1^* Z_2^* e^2}{4\pi\epsilon_0 r_{12} k_B T}, \tag{8}$$

where r_{12} is the average ion-sphere radius given by

$$r_{12} = \frac{r_1 + r_2}{2}. \tag{9}$$

In Fig. 1 we plot all these different couplings for the binary mixture of D and Ar at 100 eV as a function of Ar mole fraction. Also, in the same figure, with symbols we plot reference values for the coupling of the system computed from MD simulations as the ratio of the total average potential energy to kinetic energy. The values extracted for the coupling from the Yukawa definition, i.e. $e^{-\kappa} \Gamma_{\text{eff}}$, are the ones that most closely follow the values computed from MD on the whole range of compositions in the mixture. The values computed from Eq. (8) overestimate the coupling coefficient of asymmetric mixtures with low concentration of the high Z element by more than a factor of 7. As seen in Fig. 1 this large discrepancy is present for most of the range of composition. Only for the threshold value $\geq 40\%$ Ar mixture does Γ_{12} approach the value computed from $e^{-\kappa} \Gamma_{\text{eff}}$. This threshold value should decrease with the charge asymmetry of the mixture.

To quantify the electron fluid degeneracy we use the Ichimaru definition [38] of the electron degeneracy parameter:

$$\Theta \equiv \frac{k_B T}{E_F}. \qquad (10)$$

This parameter asymptotes to 0 as T goes to zero and/or n_e goes to infinity, in which limit the electrons are fully degenerate. It goes to infinity in the other extreme where the electrons behave as classical particles. For the system studied here the degeneracy parameter varies in the range $\Theta \in [0.5, 3]$.

B. Green-Kubo for shear viscosity

In the hydrodynamic scale the conservation equation for the momentum transfer in a finite element of fluid is given by the Navier-Stokes equation:

$$\partial_t(\rho \mathbf{v}) + \mathbf{v} \cdot \nabla(\rho \mathbf{v}) = -\nabla \cdot \overset{\leftrightarrow}{\Pi} - \nabla P + \mathbf{F}, \qquad (11)$$

where ρ is mass density, $\mathbf{v}$ is Eulerian velocity, P is total pressure and $\mathbf{F}$ includes different forces like the ones due to electric field [45, 46]. Viscosity enters as a transport coefficient in a closure for the viscous stress tensor $\overset{\leftrightarrow}{\Pi}$ in a linear response approach [15]:

$$\Pi_{ij} = -\zeta \delta_{ij}(\nabla \mathbf{v}) - \eta \left[\frac{\partial v_i}{\partial r_j} + \frac{\partial v_j}{\partial r_i} - (2/3)\delta_{ij}(\nabla \mathbf{v}) \right], \qquad (12)$$

where ζ and η are bulk and shear viscosity, respectively. In this linear approach it is assumed that the momentum flux is proportional to the magnitude of the shear stress that caused it, and η is the coefficient of proportionality. Keeping only the linear-order terms with respect to gradients in Eq. (12) corresponds to the Navier-Stokes hydrodynamics. Adding the next order gradient terms corresponds to Burnett and super-Burnett hydrodynamics [6].

In situations close to equilibrium virtual fluctuation of velocity gradient can be considered in Eqs. (11) and (12) to express the shear viscosity coefficient η as a time integral of autocorrelation function of stress tensor [45]. This is the Green-Kubo or fluctuation-dissipation approach in the context of shear viscosity. In general Green-Kubo formulas express a macroscopic phenomenological transport coefficient, like viscosity, as a time integral of microscopic time-correlation function. For shear viscosity we use the stress autocorrelation function (SAF) defined as:

$$J_{xy}(t) = \langle \sigma_{xy}(0)\sigma_{xy}(t) \rangle, \qquad (13)$$

where $\langle \cdots \rangle$ represents a statistical ensemble average, only in Section II B. The off-diagonal terms of the stress tensor σ_{xy} are given by

$$\sigma_{xy} = -\frac{1}{V_{tot}} \left(\sum_{i=1}^{N} m_i v_{x,i} v_{y,i} + \sum_i \sum_{j>i} \frac{r_{ij}^x r_{ij}^y V'(r_{ij})}{r_{ij}} \right), \qquad (14)$$

where x and y denote Cartesian coordinates, m_i is the mass of ion i and r_{ij} the distance between ions i and j, and V_{tot} the total volume of the system. The interaction force between ions i and j enters in the second term through $V'(r) \equiv dV/dr$. The first term of the stress tensor in the right hand side of Eq. (14) $\sigma_{xy,kin} = \sum_{i=1}^{N} m_i v_{x,i} v_{y,i}$, is a kinetic part that represents transverse momentum transfer by ion displacement [15, 45]. This term is important in weakly coupled plasma. For example, there would be a large contribution to this term for an ion that travels a long distance before scattering, and in that collision transfers momentum transverse to its initial motion. The second term is the potential part $\sigma_{xy,pot}$ which depends on the pair potential interaction $V(r_{ij})$. In strongly coupled plasma this becomes the dominant factor in momentum transport. Whereas the contribution to the kinetic viscosity was large for more persistent motion before scattering, this term is large for more persistent configurations with shear stress; a fluctuation induces a configuration with interionic forces that give a shear stress and that shear stress persists.

The Green-Kubo form for shear viscosity is

$$\eta = \lim_{t \to \infty} \frac{1}{nk_B T} \int_0^t d\tau J_{xy}(\tau). \qquad (15)$$

Since our MD simulations only have dynamic ions, not dynamic electrons, the Green-Kubo formula gives the ionic viscosity. Plasmas have an electronic viscosity as well, but in a weakly coupled deuterium plasma it is smaller than the ionic viscosity roughly by a factor of $\sqrt{m_e/m_D}$ and is negligible [7, 47]. As the high-Z (Ar) component is added, the ionic viscosity drops, at least initially, and the electronic viscosity becomes relatively more important. For the conditions studied here, the electronic viscosity is always less than the ionic viscosity and it is relatively well understood, so we will ignore it.

We make use of some properties of the plasma to improve the statistical convergence of the viscosity calculation. For the isotropic three dimensional case we can make use of invariance under 90 degree rotations to deduce that $J_{xy}(t) = J_{xz}(t) = J_{yz}(t) \equiv J(t)$. Two other independent components of shear stress tensor can be constructed as differences of the diagonal terms [20, 48]. Therefore we can get good statistics in extracting the value of the SAF by averaging over five components of the shear stress tensor.

It will be useful to separate the SAF in terms of three components: a kinetic $J_{xy,kin} \equiv \langle \sigma_{xy,kin}(0)\sigma_{xy,kin}(t) \rangle$, a potential $J_{xy,pot} \equiv \langle \sigma_{xy,pot}(0)\sigma_{xy,pot}(t) \rangle$ and a cross term given by $J_{xy,cross} \equiv \langle \sigma_{xy,pot}(0)\sigma_{xy,kin}(t) \rangle$. This enables us to write the shear viscosity as a sum of three terms:

$\eta = \eta_{\text{kin}} + \eta_{\text{pot}} + \eta_{\text{cross}}$ each of which is given by

$$\eta_{\text{kin}} = \lim_{t \to \infty} \frac{1}{nk_BT} \int_0^t d\tau \, \langle \sigma_{\text{xy,kin}}(0)\sigma_{\text{xy,kin}}(\tau) \rangle \quad (16)$$

$$\eta_{\text{pot}} = \lim_{t \to \infty} \frac{1}{nk_BT} \int_0^t d\tau \, \langle \sigma_{\text{xy,pot}}(0)\sigma_{\text{xy,pot}}(\tau) \rangle \quad (17)$$

$$\eta_{\text{cross}} = \lim_{t \to \infty} \frac{2}{nk_BT} \int_0^t d\tau \, \langle \sigma_{\text{xy,pot}}(0)\sigma_{\text{xy,kin}}(\tau) \rangle \,. \quad (18)$$

C.   Details of the MD simulations

To calculate shear viscosity of a binary mixed plasma of D with Ar we have performed MD simulations at temperatures $T = 100$, 200 and 500 eV, and ion number density 10^{25}/cc. We input the ionization as a free parameter independent of the thermodynamic conditions of the mixtures. The physical ionization can be determined by an average atom Thomas-Fermi approximation, but we keep it as an adjustable parameter. We impose that the deuterium is fully ionized, $Z_{\text{D}}^* = 1$, and the ionization of Ar is $Z_{\text{Ar}}^* = 13$, which are close to the values computed from average atom Thomas-Fermi technique [9]. The screening length that enters the Yukawa ion-ion potential was computed by using relation (2). For each of the above conditions we also consider mixtures whose Ar mole fraction is $X = 0.01$, 0.05, 0.1, 0.2 and 0.5. The calculations were performed with enough ions ($30000 \leq N \leq 120000$) over long enough time scales to ensure convergence with insignificant statistical uncertainty (less than 5%).

The screening length sets an important length scale for the system. When the screening is strong ($\kappa \geq 1$), the Yukawa potential is short ranged. In this case it is computationally advantageous to introduce a cutoff for the interaction potential, limiting the need to sum pairwise ion-ion interactions only to those ions situated within the (κ-dependent) cutoff radius.

The MD simulations [49] presented here are initiated from a spatially random ion configuration, and ion velocities sampled from a Maxwellian distribution at a given temperature. The random configuration of the ions of each component ensures a spatially uniform mixture as well, suitable for equilibrium MD. The system is initially equilibrated at the desired temperature using a Nosé-Hoover [50–52] thermostat (constant number of ions N, volume V and temperature T). Typically the system is left to equilibrate for 50000 timesteps in this NVT ensemble. The subsequent production run to calculate the stress tensor is done in a microcanonical ensemble with constant N, V and total energy E.

The time scale of the system is set by the ionic plasma frequency

$$\omega_p = \sqrt{\frac{e^2 \langle Z^* \rangle^2 n}{\epsilon_0 \langle m \rangle}}. \quad (19)$$

The timestep in the runs was taken as $\Delta t \simeq 1/(\varpi\omega_E)$, where ω_E is the Einstein frequency, that physically de-

scribes the oscillatory motion of a caged ion in the well potential created by its neighbors, and the coefficient ϖ had values in the range $100 \leq \varpi \leq 1000$. The values of ϖ were chosen such that the timestep is small enough to accurately resolve the trajectory of ion through collisions. Usually the value of $\varpi = 300$ was used; however, in the cases with $T = 500$ eV, $X \leq 0.1$ and $Z_{\text{Ar}} = 13$, we needed to reduce the timestep by a factor of ten ($\varpi = 1000$) to resolve strong binary collision events. A more efficient method along the lines of the Kepler predictor algorithm [53], that allows for an improved integration of the occasional close-encounter collisions, could enable the use of a longer timestep at high T. We use the following form for the Einstein frequency [19]:

$$\omega_E(\kappa) = \sqrt{\frac{1}{3}}\omega_p \exp(-0.2\kappa^{1.62}) \quad (20)$$

fitted to the Ohta and Hamaguchi MD results [4] accounting for screening. In the limit of no screening $\kappa \to 0$, the above reduces to $\omega_E = \omega_p/\sqrt{3}$. For the conditions studied here the values of ω_E span a range from $\omega_{E,min} \sim 1.683$ fs^{-1} for mixtures with 1% Ar at 100 eV, to $\omega_{E,max} \sim 3.272$ fs^{-1} for mixtures with 50% Ar at 500 eV. The timestep needed to ensure conservation of energy in the MD was as low as 10^{-4} fs.

The production MD runs in an NVE ensemble were executed for 2×10^7 timesteps for each case and the components of stress tensor were recorded. The production run was separated over blocks of $t_{max} \sim 10^5$ timesteps, so that the results on different blocks are not correlated. SAF correlation functions were computed over each block and their average, corresponding to a time average, was saved as a table over the time span t_{max}.

III.   MOLECULAR DYNAMICS SIMULATION RESULTS

In Fig. 2 we present plots of the SAF for different compositions at 200 eV. The ionizations of deuterium and argon were kept constant at 1 and 13, respectively, while the composition of the binary mixture varied from 1% to 50% argon mole fraction. The ion number density was 10^{25} ion/cm^3. In this figure we specifically plot SAF as function of time for mixtures with Ar mole fraction $X = 0.1$, 0.2 and 0.5.

The correlation functions are expected to decay exponentially initially and switch to slower power law decay at long times due to memory effects and hydrodynamic modes [45, 54]. As seen by the nearly straight-line decrease in the log plot in Fig. 2, these correlation functions decay exponentially to 2 fs or more depending on the mixture. Beyond that time fluctuations in the tail of the SAF obscure the form of its long-time decay due to the high temperature. Nevertheless, it is clear that the contribution from the long-time tail is insignificant ($< 2\%$), and we can make the approximation that the correlation function continues to decay exponentially for
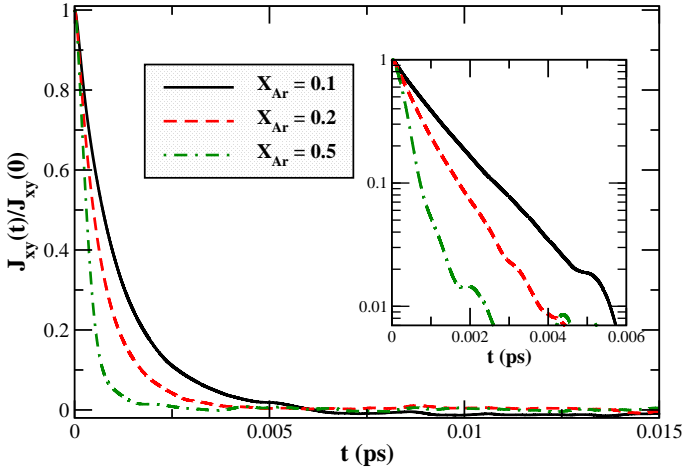
FIG. 2. (Color online) The stress autocorrelation function SAF as a function of time that enters in the shear viscosity plotted for different compositions of binary ionic mixture at 200 eV and 10^{25} ions/cc. In the inset same results are plotted in log scale. SAF were calculated out to a time 40 fs (not shown).
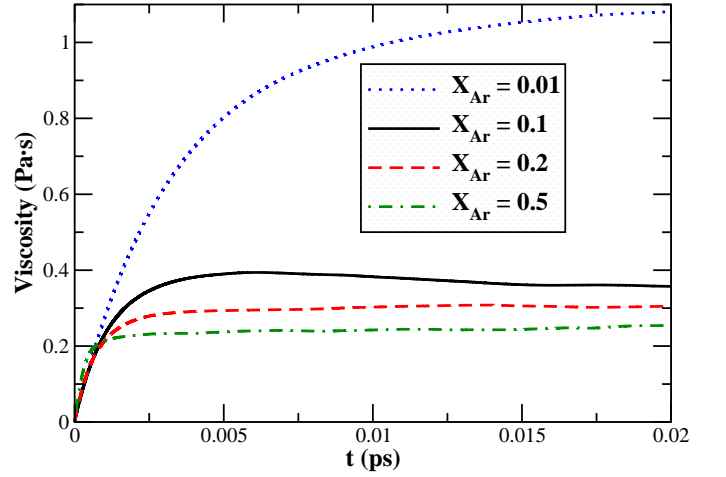

FIG. 3. (Color online) Partial integrals in time of the correlation functions shown in Fig. 2. These are the average over different initial conditions of the cumulative sums of the SAF, as highlighted in Fig. 4, for each respective case. Each SAF was calculated out to a time of 40 fs (not shown).

all time. In practice, we have fit the tail and carried out this extrapolation in the partial integrals of the viscosity.

In Fig. 3 the partial integrals, or more precisely the cumulative sums, of SAF are shown as a function of time. The cumulative sums were computed from MD by post-processing as:

$$\eta_{cum}(t) = \left[\sum_k^{t/\Delta t} a_k \Delta t J(t_k) \right]. \tag{21}$$

where the coefficients a_k give the Simpson's rule approximation to the integral.

These are fit with

$$\eta_{cum}(t) = \eta_{fit} \left[1 - \exp\left(-\frac{t}{\tau_c} \right) \right]. \tag{22}$$

The value extracted η_{fit} is what we report as the shear viscosity computed from MD. The cumulative sums will asymptote to slightly different values of η_{fit} for different runs. For each case studied we considered five different initial configurations in order to calculate an error bar. This variation is shown in Fig. 4 for a particular case with $X_{Ar} = 0.1$ and $T = 200$ eV.

Finally in Table I the complete results of MD for the range of molar composition of Ar between 0.01 and 0.5, and for $T = 100$, 200 and 500 eV, in ion density 10^{25} ion/cc are shown. These results are then plotted with symbols in Fig. 5. It is interesting that for the highest temperatures $T = 200$ and 500 eV viscosity is monotonically dropping with Ar composition. This trend is an indication that for this range of T the mixtures remain weakly coupled with the shear viscosity dominated by the kinetic contribution.
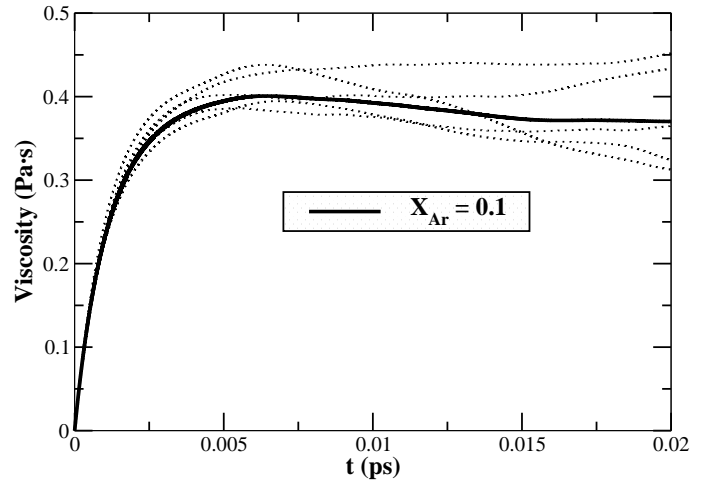

FIG. 4. (Color online) The partial integrals in time of SAF for five different initial configurations represent with dotted lines. The solid line is the average. This particular case corresponds to a mixture with 10% Ar at T=200 eV. The viscosity is found to be 0.3706±0.033 Pa·s.

This behavior changes for more strongly coupled plasmas. Specifically, at 100 eV, the viscosity decays with the increase of Ar mole fraction until it reaches a minimum at $X_{Ar} = 0.2$, after which it increases with Ar composition. This correspond to a transition in the nature of the momentum transfer, from a fully kinetic regime at very low Ar composition to being dominated by potential and cross terms at $X_{Ar} > 0.1$. This transition is clearly demonstrated in Table II and Fig. 6 where we plot the total shear viscosity with black dot symbols and the kinetic component of shear viscosity with red square

TABLE I. Shear viscosity values computed from MD for binary mixtures of deuterium and argon at $T = 100, 200$ and 500 eV with Ar mole fraction $X_{\text{Ar}} = 0.01, 0.05, 0.1, 0.2$ and 0.5, at a density $n = 10^{25}$ ion/cc. Values of the effective Coulomb coupling Γ_{eff}, along with screening κ and mass density ρ are also shown.

T (eV)	X_{Ar}	η (Pa·s)	Γ_{eff}	κ	ρ(g/cc)
	0.01	0.3483 ± 0.0135	0.8874	1.0329	39.744
	0.05	0.2349 ± 0.0124	2.6577	1.1425	64.939
100	0.1	0.1695 ± 0.0067	5.2603	1.2377	96.432
	0.2	0.1490 ± 0.0091	11.4114	1.3644	159.42
	0.5	0.1781 ± 0.0067	34.8578	1.5723	348.38
	0.01	1.0675 ± 0.081	0.4437	0.8472	39.744
	0.05	0.5984 ± 0.062	1.3289	0.9748	64.939
200	0.1	0.3706 ± 0.033	2.6301	1.0927	96.432
	0.2	0.2996 ± 0.026	5.70572	1.2544	159.42
	0.5	0.2493 ± 0.017	17.4289	1.5130	348.38
	0.01	5.9345 ± 0.562	0.1775	0.5714	39.744
	0.05	2.4632 ± 0.148	0.5315	0.6773	64.939
500	0.1	1.5905 ± 0.034	1.0521	0.7853	96.432
	0.2	0.9496 ± 0.139	2.28229	0.9533	159.42
	0.5	0.5081 ± 0.034	6.97155	1.2726	348.38

TABLE II. Shear viscosity values η and its kinetic component η_{kin} computed from MD for binary mixtures of deuterium and argon at $T = 100$ eV and density $n = 10^{25}$ ion/cc. Values of Yukawa coupling are shown in the last column.

X_{Ar}	η (Pa·s)	η_{kin} (Pa·s)	$e^{-\kappa}\Gamma_{\text{eff}}$
0.05	0.2349 ± 0.0124	0.2393 ± 0.0049	0.8479
0.1	0.1695 ± 0.0067	0.1699 ± 0.0048	1.5258
0.2	0.1490 ± 0.0091	0.1220 ± 0.0032	2.9161
0.5	0.1781 ± 0.0067	0.0818 ± 0.0014	7.2355

symbols. It is clear that up to $X_{\text{Ar}} = 0.1$ the kinetic term dominates the shear viscosity.

IV. WEAKLY COUPLED REGIME

In the weak coupling limit, the transport coefficients including viscosity have been expressed through binary collision frequencies that enter in Boltzmann kinetic equation for the velocity distribution function $f_i(\mathbf{v})$. For one component plasma (OCP) in this limit, i.e. $\Gamma \ll 1$, with Coulomb interactions among the ions and using the Landau collision operator, the reduced viscosity is [55–58]:

$$\eta_L^* \equiv \eta/\eta_0 = \frac{5}{6}\sqrt{\frac{\pi}{3}}\frac{1}{\Gamma^{5/2}\ln\Lambda}, \qquad (23)$$

where the characteristic viscosity η_0 is defined as

$$\eta_0 \equiv mnr_{ws}^2\omega_p. \qquad (24)$$

Here ω_p is the plasma frequency (19) and $\ln\Lambda = -\ln\left(\sqrt{3}\Gamma^{3/2}\right)$ is the Coulomb logarithm. More generally following either the Chapman-Cowling [6] or Burgers method [59] we can express viscosity, as well as other linear transport coefficients, through the so-called collision integrals $\Omega_{ij}^{(lk)}$ that are linearly proportional to the binary collision frequency among particles of species i and j. The collision integrals can be computed numerically or analytically for different interaction potentials. A more detailed description can be found in Appendix A.

For plasmas with one ionic species, the first approximation in the expansion of distribution function around the Maxwellian gives the following expression for the shear viscosity coefficient [6, 59]:

$$[\eta_i]_1 = \frac{5k_BT}{8\Omega_{ii}^{(22)}}, \qquad (25)$$

where $\Omega_{ii}^{(22)}$ is the Chapman-Enskog second-order momentum collision integral among ions of the same species i. In the OCP case with Coulomb interactions the collision integral may be calculated to give

$$[\eta^*]_1 = \frac{5\sqrt{\pi}}{3\sqrt{3}\Gamma^{5/2}\mathcal{F}_{ii}^{(22)}}, \qquad (26)$$

where $\mathcal{F}_{ij}^{(lk)}$ is a generalized Coulomb logarithm [60, 61] given in Eq. (A6). In the low coupling limit this asymptotically matches the Landau $\ln\Lambda$. Referring to the relation of $\mathcal{F}_{ij}^{(lk)}$ to the Landau-Spitzer Coulomb logarithm given in the Appendix (A7) and taking $l = k = 2$, it can be shown that Eq. (26) reduces to the Landau form of viscosity in Eq. (23).
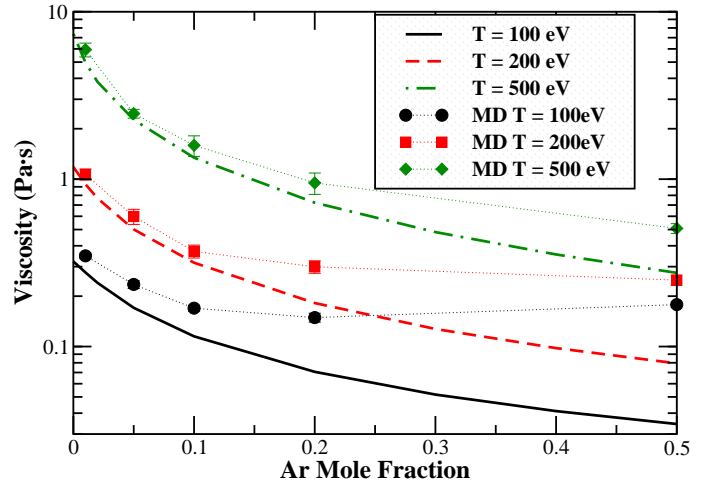

FIG. 5. (Color online) Viscosity versus composition for $T = 100, 200$ and 500 eV. The MD results are shown with symbols compared to the viscosity calculated from Chapman-Enskog collision integrals shown without symbols.

In the first Enskog approximation the viscosity for binary mixtures $[\eta]_1$ is given in Section 9.84 of Chapman

and Cowling [6]:

$$[\eta]_1 = \frac{\alpha_{ij} + \alpha_{ji} + \frac{E}{2[\eta_i]_1} + \frac{E}{2[\eta_j]_1} + \frac{4}{3} - 2A}{\frac{\alpha_{ij}}{[\eta_i]_1} + \frac{\alpha_{ji}}{[\eta_j]_1} + \frac{E}{2[\eta_i]_1[\eta_j]_1} + \frac{4A(m_i+m_j)^2}{3Em_im_j}}, \quad (27)$$

where i and j indicate the two different species and

$$E \equiv \frac{kT(m_i + m_j)^2}{8m_im_j\Omega_{ij}^{(11)}}, \quad (28)$$

$$A \equiv \frac{\Omega_{ij}^{(22)}}{5\Omega_{ij}^{(11)}}, \quad (29)$$

with $[\eta_i]_1$ representing the viscosity of component i as computed from Eq. (25) using the mixed plasma screening length described below (31). Also,

$$\alpha_{ij} = n_{ij}\left(\frac{2}{3} + \frac{m_i}{m_j}A\right), \quad (30)$$

where $n_{ij} \equiv X_i/X_j$.

In Appendix B we provide a similar form in terms of Burgers [59] resistant and ratios coefficients. Also, in Appendix B a simplified approximation of multicomponent mixture viscosity is described that is well-suited for use in hydrodynamic codes. It agrees well with Eq. (27) for the binary mixture cases studied here. More details on this choice are explained in Appendix B.

As seen from Eq. (27) the value of shear viscosity in mixtures in the first Enskog approach depends on all collision integrals $\Omega_{ij}^{(lk)}$ with $l, k \leq 2$. This point is discussed further in Appendix B, where it is shown that two rank-2 scattering integrals make the most significant contribution, so even in an approximate sense the mapping of the shear viscosity to Landau's $\ln\Lambda$ is not one-to-one. This relationship is different from the one for interdiffusion in a weakly coupled binary mixture which depends only on one collision integral $\Omega_{ij}^{(11)}$, the rank-1 collision integral among the two species [9].

To compute the collision integrals that enter in Eq. (27), we use the effective Yukawa interaction (1) among the ions [3]. To include collective effects from other particles, a Lenard-Balescu approach [62, 63] that introduces a dynamical screening coefficient in an effective pairwise potential can be used to some extent. This dynamical screening is due to other particles and it is different from the screening that each ion experiences due to its electron cloud. The effective pairwise potential can be used to compute the collision integrals [60].

For situations close to equilibrium, as the one studied in the Green-Kubo approach, only low frequency components of the dynamic screening due to other ions significantly contribute to the transport coefficient. As a consequence an adiabatic approach [64] along the lines of Paquette et al. [3] is suitable to compute collision integrals that determine the transport coefficients of ions.

As in our previous work on diffusion [9] we adapt the work of Paquete et al. [3] to compute the shear viscosity. We use the Yukawa potential to compute the collision integrals $\Omega_{ij}^{(lk)}$ with a screening coefficient λ that
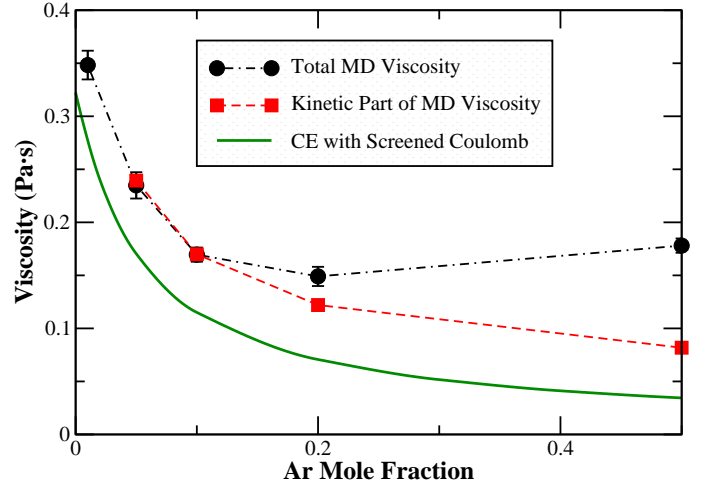

FIG. 6. (Color online) Shear viscosity versus composition for $T = 100$ eV at 10^{25} ion/cc, as computed from the Chapman-Enskog collision integrals using the tabular values in Paquette et al. [3]. With black circular symbols results from the MD simulations for the full shear viscosity are presented. The kinetic component of the shear viscosity are presented by red square symbols.

interpolates between the total Debye screening λ_D and Wigner-Seitz radius r_{ws} by

$$\lambda = \sqrt{(\lambda_D^2 + r_{ws}^2)}. \quad (31)$$

The total Debye screening includes ions as well as electrons and is given by

$$\lambda_D = \frac{1}{\sqrt{\lambda_{D,i}^{-2} + \lambda_{D,e}^{-2}}}, \quad (32)$$

where $\lambda_{D,i} = \sqrt{(\epsilon_0 k_B T)/(n\langle Z^2\rangle e^2)}$ is the screening due to ions and $\lambda_{D,e}$ the screening of the electrons expressed by Eq. (2). The screening $\lambda_{D,e}$ accounts for the electron partial degeneracy. For a given state (X, n, T, Z_1^*, Z_2^*) the same value of screening λ is used in the Paquette tables [3] to compute all of the collision integrals, whether for like species, $\Omega_{ii}^{(lk)}$, or different species, $\Omega_{ij}^{(lk)}$.

We compare the results from these kinetics model calculations with the viscosity calculated from MD in Fig. 5. The MD uses a Yukawa interaction based on $\lambda_{D,e}$ alone since the other contributions to λ in the kinetics model account for ion correlations that the MD simulates explicitly. We see a good agreement at $T = 500$ eV for argon content up to $X_{Ar} = 0.2$, with errors less than 50%. The discrepancy is greater for higher Ar mole fractions and for lower temperatures. At fixed number density, increasing the Ar mole fraction and decreasing the temperature increases the plasma coupling of the mixture. In the more strongly coupled plasmas, the kinetic part of viscosity decreases, while the potential and cross term contributions to the viscosity increase.

While MD inherently accounts for all these contributions, the kinetic theory based on binary collisions can only compute the kinetic part [21]. This limitation is related to the fact that the binary collision operator considered in the Boltzmann equation does not account for the contribution to transport coefficients from the potential energy of the ions. As such this theory can describe only that part of the momentum transfer mediated by the particles displacement.

As shown in Fig. 6 the results from the kinetic computations qualitatively describe the change with composition of the kinetic part of the shear viscosity. The quantitative discrepancy between the kinetic part computed from MD with the shear viscosity computed by kinetic theory is due to the fact that at $T = 100$ eV the mixture is weakly to moderately coupled with the coupling on the order of unity as seen in Fig. 1.

V. MIXING RULES

In what follows we describe some mixing schemes that compute shear viscosity of the mixture in terms of that of its component. We compare the predictions of those mixing rules with our MD results.

A. Binary Ionic Mixture for rigid electron background

Bastea [24] developed a mixing scheme for BIM systems where the ions interact via a Coulomb potential with a rigid neutralizing electron background. In his approach Bastea made use of effective medium theories by assigning to each ion a volume that is related to the ion-sphere. The effective viscosity of the binary mixture η_m was determined using the following relation:

$$\Psi_1 \frac{\eta_1 - \eta_m}{\eta_1 + 1.5\eta_m} = \Psi_2 \frac{\eta_m - \eta_2}{\eta_2 + 1.5\eta_m}, \qquad (33)$$

where Ψ_i is the volume fraction of species i, which in the ion-sphere model is given by: $\Psi_i \equiv X_i Z_i^* / \langle Z^* \rangle$. This form of mixing rule interpolates between values of the viscosity of each component based on the OCP model that he built from his MD results given by:

$$\eta_i = \eta_{0i} \left(0.482 \Gamma_i^{-2} + 0.629 \Gamma_i^{-0.878} + 0.00188 \Gamma_i \right), \quad (34)$$

where $\eta_{0i} \equiv n_i m_i r_{ws}^2 \omega_{p,i}$. The plasma frequency of each species is

$$\omega_{p,i} = \sqrt{\frac{e^2 \left(Z_i^* \right)^2 n_i}{\epsilon_0 m_i}}, \qquad (35)$$

and the Coulomb coupling Γ_i of each component i that enters in Eq. (34) is given by Eq. (6). We plot with a green dot-dashed line results from this analysis in Fig. 7.

In the same plot results from MD are shown with symbols.

As the Ar mole fraction increases the shear viscosity decreases while the mixture remains in the kinetic regime. This decrease is related to the fact that the effective coupling of the mixture increases as the number of Ar atoms increases. After about 15-20% Ar the viscosity value reaches a minimum and increases again. This change corresponds to a transition from the kinetic to potential dominated regime. The corresponding Coulomb effective coupling where this transition occurs and where shear viscosity reaches its minimum is at $\Gamma_{\rm eff} \sim 8 - 11$. This behavior is qualitatively captured by using Bastea mixture rule. However, the value where this transition is observed is at a much lower value of Ar composition.

Quantitatively, there is substantial discrepancy between MD and the Bastea mixing rule for almost the whole range of composition. The main factor for this discrepancy is the fact that the MD in this work accounts for the polarizability of the free electron fluid, whereas Bastea built his model for binary ionic mixtures immersed in a rigid electron background. He also showed [24] that this mixing rule describes well MD results for a system whose particles interact by pure Coulomb potential. A main outcome from this comparison is the fact that electron polarizability significantly affects the values computed for shear viscosity. Taking into account the electron screening results in a weaker coupled plasma. Therefore the transition from a kinetic to a potential dominated regime of η occurs at a higher mole fraction of the high Z material. This explains the large discrepancy on the value X_{min} of the high Z component fraction where Bastea mixing rule predicts the minimum of η versus our MD results. It also explains the fact that this mixing rule underestimate by a factor of two the value of η at mixtures with $X_{\rm Ar} < 10\%$ where the kinetic term is dominant.

B. Tanaka-Ichimaru approach in the screened OCP model for dense plasmas

We next compare our MD against shear viscosity models that were developed for plasmas accounting for the polarizable electron background (screening). One of the first such studies for dense plasmas was carried by Tanaka and Ichimaru [65] (TI) assuming a screened Coulomb interaction among the ions. They carried out Lenard-Balescu calculations of the viscosity of the plasma including local field corrections to extend the Lenard-Balescu description of the weakly coupled plasmas to moderate coupling. Using hypernetted chain to determine the radial distribution functions, they computed the reduced shear viscosity including the generalized Coulomb logarithm $\mathcal{F}(\Gamma, \Theta)$:

$$\eta_{TI}^* = \frac{5}{6} \sqrt{\frac{\pi}{3}} \frac{1}{\Gamma^{5/2} \mathcal{F}(\Gamma, \Theta)}, \qquad (36)$$
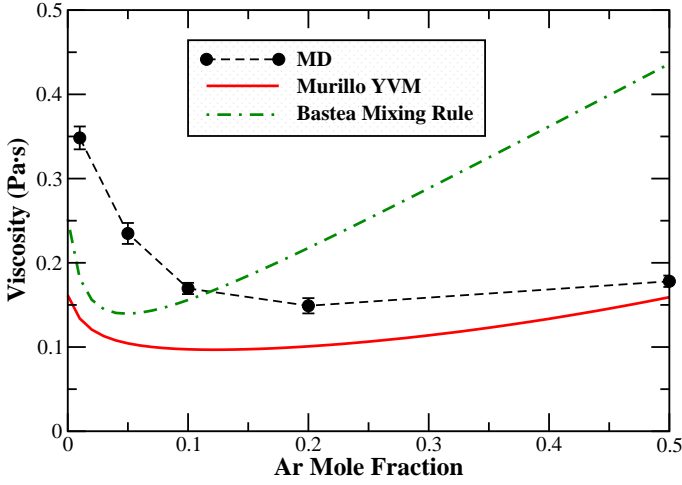
FIG. 7. (Color online) Shear viscosity of a mixed D-Ar system from MD at T=100 eV and ion density 10^{25} ion/cc. The charge of D and Ar are respectively $Z_D = 1$ and $Z_{Ar} = 13$. The results from MD are shown with symbols. Estimates from Bastea mixing model are shown with the green dot-dashed line. Results from the extension to mixtures of the Murillo's YVM prescription are shown with the solid red line.

where $\mathcal{F}(\Gamma, \Theta)$ is parametrized by:

$$\mathcal{F}(\Gamma, \Theta) = \frac{-1.5 \ln \Gamma + a(\Theta) + b(\Theta)\Gamma}{1 + c(\Theta)\Gamma^{5/2}}. \quad (37)$$

As usual Γ is the Coulomb coupling and Θ the electron degeneracy (10). The parameters $a(\Theta), b(\Theta)$ and $c(\Theta)$ were fitted in Ref. [65] with Padé approximations to a limit range of thermodynamics conditions that correspond to values of $\Theta = 0.1, 1, 10$ and $\Gamma = 0.1, 0.2, 0.5, 1$ and 2.

To extend this model to a binary mixture akin to the one studied in this article we use the effective one-fluid mixing rule of mapping $\Gamma \to \Gamma_{\text{eff}}$. This approach has also been used previously for shear viscosity [19, 24, 56]. Plugging the Γ_{eff} and Θ to Eq. (36) and using the hydrodynamic plasma mixture frequency ω_p in Eq. (19) we extract values of shear viscosity from this extended TI model. Values from this analysis are shown in Table III along with the computed values from our MD. In this Table we have highlighted in gray those rows that correspond to cases for which the value of Γ_{eff} and Θ fall within the range used to build the TI model.

The agreement between MD and the extended TI model is within 50% for the cases highlighted, with larger errors for some of the other cases. There are two main factors that contribute to the discrepancy: i) the fact that the table of the values of Γ and Θ upon which TI is built is sparse, and ii) the interpolation form in Eq. (2) that we used in order to extract the screening coefficients due to electron polarizability may not very accurately account for the electron-ion correlations. An improvement on both these issues is beyond the scope of this paper.

TABLE III. Shear viscosity values computed from MD for binary mixtures of deuterium and argon and from Tanaka Ichimaru local field correction approach in Eq. (36) replacing Γ with Γ_{eff}. In the second column X_{Ar} denotes Ar mole fraction. The values of coupling Γ_{eff} and electron degeneracy Θ are shown in fourth and fifth column, respectively. We have highlighted in gray those rows that correspond to cases for which the value of Γ_{eff} and Θ fall within the range that the extended Tanaka-Ichimaru model was built.

T (eV)	X_{Ar}	η_{MD} (Pa·s)	η_{TI} (Pa·s)	Γ_{eff}	Θ
100	0.01	0.3483 ± 0.0135	0.2969	0.8874	0.5478
	0.05	0.2349 ± 0.0124	0.1394	2.6577	0.4319
	0.1	0.1695 ± 0.0067	0.0989	5.2603	0.3493
	0.2	0.1490 ± 0.0091	0.0729	11.4114	0.2613
	0.5	0.1781 ± 0.0067	0.0519	34.8578	0.1615
200	0.01	1.0675 ± 0.081	0.9295	0.4437	1.0957
	0.05	0.5984 ± 0.062	0.3934	1.3289	0.8638
	0.1	0.3706 ± 0.033	0.2626	2.6301	0.6986
	0.2	0.2996 ± 0.026	0.1830	5.7057	0.5226
	0.5	0.2493 ± 0.017	0.1229	17.4289	0.3229
500	0.01	5.9345 ± 0.562	4.6869	0.1775	2.7392
	0.05	2.4632 ± 0.148	1.62398	0.5315	2.1595
	0.1	1.5905 ± 0.034	1.0136	1.0521	1.7464
	0.2	0.9496 ± 0.139	0.6534	2.2823	1.3065
	0.5	0.5081 ± 0.034	0.4040	6.9716	0.8073

C. Yukawa Viscosity Model and its extension to mixtures

The TI model presented in the previous section is less practical for computation of transport coefficients for systems where the ions interact with an effective screened Yukawa potential. A thorough parametric study of viscosity for one component Yukawa systems was conducted by Saigo and Hamaguchi [17] and Salin and Caillol [25]. The authors explored different values of the pair (Γ, κ) and used MD to extract the shear viscosity values. The two works are complimentary to each other in terms of the (Γ, κ) space that they covered.

Murillo has developed a model for the viscosity of single-species Yukawa systems [19], the Yukawa Viscosity Model (YVM), motivated by an interest in predicting the viscosity of liquid metals and warm dense matter. He based his model on the results from the MD study of Saigo and Hamaguchi [17]. YVM expresses the viscosity η_{YVM} in terms of a reference viscosity $\hat{\eta}_0$, the plasma coupling Γ, and the plasma coupling at melt, $\Gamma_m(\kappa)$:

$$\eta_{YVM} = \hat{\eta}_0 \left(a(\kappa) \frac{\Gamma_m}{\Gamma} + b(\kappa) \frac{\Gamma}{\Gamma_m} + c(\kappa) \right), \quad (38)$$

where the coefficients a, b and c are κ-dependent. This dependence is in general very weak [17], which allowed fitting over the cases $\kappa = 2$ and 3 and extracting the following average numbers for these parameters: $a = 0.0051$,

$b = 0.374$ and $c = 0.022$. The characteristic viscosity $\hat{\eta}_0$ is:

$$\hat{\eta}_0 = \sqrt{3}\omega_E m n r_{ws}^2, \qquad (39)$$

where ω_E is the Einstein frequency given by Eq. (20), explicitly

$$\hat{\eta}_0 = \sqrt{\frac{m\,(Z^*)^2 e^2 n}{\varepsilon_0}}\, n\, r_{ws}^2 \exp\left(-0.2\kappa^{1.62}\right) \qquad (40)$$

$$= \sqrt{3m\Gamma\, k_B T}\, n\, r_{ws} \exp\left(-0.2\kappa^{1.62}\right). \qquad (41)$$

The expression for Γ_m:

$$\Gamma_m(\kappa) = \Gamma_m(0) + 82.8 \exp\left(0.565\kappa^{1.38} - 1\right) \qquad (42)$$

is a refitting of the Yukawa MD melt values from Hamaguchi, Farouki and Dubin [66]. The value of coupling at melt for an OCP system at $\kappa = 0$ is $\Gamma_m(0) = 171.8$. Equations (38) and (40) were obtained by fitting to Yukawa MD calculations of viscosity by Saigo and Hamaguchi [17]. These MD calculations were done for values of Γ ranging in the range $2 - 1000$ and values of the screening κ in the range $0.1 - 3$. The YVM model gave a good description of the MD results over this range of Γ. It was also suggested [19] that although the YVM model was built to fit the above range of Γ for $\kappa = 2$ and 3, it can still describe systems with other values of κ close to the above values. In this range the YVM model provides accurate values of shear viscosity of liquid metals at the conditions that it was meant to describe. To extend this model to the limit of very hot plasmas, in which case both Γ and κ go to 0, Rudd [67] developed an extended YVM (eYVM) model. We provide some details of this model at Appendix C and refer the interested reader to Ref [67].

We adapt the YVM to mixtures by using the one-fluid mixing rule of mapping Γ_{eff} to Γ, as well as mapping $\langle m \rangle$ to m. Replacing Γ and m with Γ_{eff} and $\langle m \rangle$, respectively, in Eq. (38) we extract the values of viscosity from this mixing rule. These are plotted with solid red line in Fig. 7. As expected YVM is in fairly good agreement with the MD results at 100 eV for mixtures with more than 10% Ar. Referring to Table I these correspond to mixtures with $\Gamma_{\text{eff}} > 5$ and $\kappa > 1.2$. The agreement gets better as the Ar mole fraction is increased and as the temperature is decreased. This stresses the fact that YVM describes well moderately to strongly coupled plasmas where the potential and cross term in the shear viscosity are dominant. The model fails to describe accurately the MD results for low Ar mole fraction and for higher T, where the plasma is weakly coupled and the viscosity is dominated from the kinetic component of momentum transfer. In the next Section we extend the YVM for mixtures to the weakly coupled regime. This approach is analogous to the eYVM model that Rudd [67] developed for pure Yukawa systems.

D. Hybrid kinetics-MD viscosity model for mixtures

A hybrid Kinetics-Molecular Dynamics (KMD) viscosity model for plasma developed for hydrodynamic codes blends Murillo's YVM with the mixture viscosity from kinetic theory using (27) for binary mixtures. Taking advantage of the behavior that the viscosity from the kinetic model is larger for weak coupling and viscosity from YVM is larger for strong coupling, the blend smoothly transitions from the regime where one is larger to the regime where the other is larger:

$$\eta_{KMD} \approx \left([\eta]_1^2 + \eta_{YVM}^2\right)^{1/2}. \qquad (43)$$

This model represents in an approximate fashion contribution of the kinetics, cross and potential terms of viscosity. A more physically based blend could also be constructed using the coupling parameter Γ like the approach in Appendix C. As discussed previously the mixture viscosity η_{YVM} is evaluated from the YVM given in Eqs. (38) and (40) with Γ and m replaced by Γ_{eff} and $\langle m \rangle$, respectively. The results of this hybrid YVM-Paquette model are shown in Fig. 8 compared with the MD results, showing reasonably good agreement (within 16%) for all temperatures and mixtures tested. This ap-
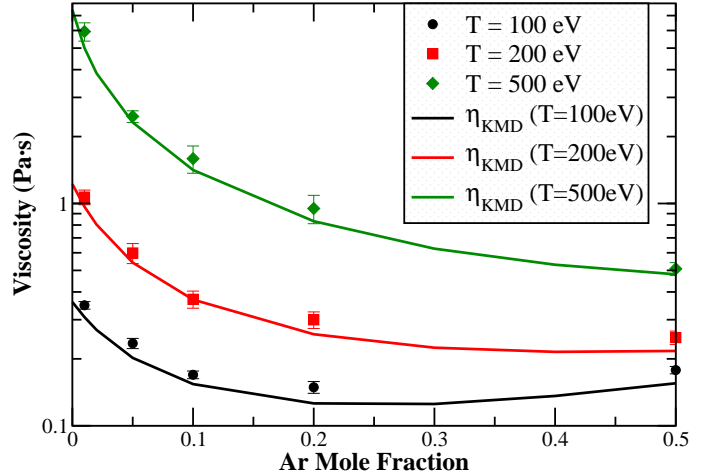

FIG. 8. (Color online) Viscosity for a deuterium-argon mixture at temperatures 100, 200 and 500 eV and ion density $n = 10^{25}$ ion/cc. The MD values of the shear viscosity η are plotted with symbols. The solid lines represents values of viscosity η_{KMD} computed by the KMD viscosity model in Eq. (43). This model represents in an approximate fashion contribution of the kinetics, cross and potential terms of viscosity. Results from the KMD model and from the equilibrium MD are in good agreement (within 16%) over the aforementioned conditions.

proach can be extended to multi-component mixtures by using a more general formula (B10) for $[\eta]_1$ given in the Appendix B.

VI. SUMMARY

In this Article we have presented results from an MD study of shear viscosity in binary asymmetric mixture of dense plasmas. The focus was mixtures of D and Ar at $T = 100$, 200 and 500 eV and at the number density of 10^{25} ions/cm^3. We considered the system as described by Yukawa interionic potential which effectively describes the adiabatic screening of the ionic charge from the free electron cloud. This approach is reasonable at the range of the thermodynamic conditions studied here. We used the Green-Kubo approach to extract the value of shear viscosity from equilibrium MD runs. For the runs executed at 100 eV the computed viscosity decreases at low mole fraction of Ar and increases at higher mole fraction. This corresponds to a transition in the nature of momentum transfer from purely kinetic at low Ar to potential at higher Ar composition. It also reflects the change of viscosity with the coupling of the system for moderate to strongly coupled plasmas. At the higher temperatures, 200 and 500 eV, the plasma remains weakly coupled and the aforementioned transition does not occur. As a result the viscosity only decreases with Ar mole fraction. For mixtures with less than 10% Ar at 500 eV, which correspond to plasma with the lowest coupling studied here, viscosity computed from MD compares very well with values computed from Chapman-Enskog kinetic theories. At lower temperatures and higher Ar composition, which corresponds to more strongly coupled plasma, these kinetic theories do not agree well with MD. To this end we developed a simple hybrid model that interpolates between a kinetic model, the Burgers viscosity using the Paquette collision integrals, at weak coupling and the Murillo Yukawa viscosity model at strong coupling. The hybrid model compares well with the MD results over the whole range of thermodynamic conditions studied here. The model is generic and it should work well for different binary mixtures from moderately strong to weak coupling. Its applicability can be extended to multicomponent mixtures.

ACKNOWLEDGMENTS

Appendix A: Chapman-Enskog Collision Integrals

This appendix provides a brief overview of collision integrals. In the Chapman-Enskog approach the transport coefficients are computed using collision integrals, which are related to the differential cross sections of a classical binary collision, integrated over a Maxwellian velocity distribution. The collision integrals are given by [3, 6]:

$$\Omega_{ij}^{(lk)} = \sqrt{\frac{k_B T}{2\pi m_{red}}} \int_0^\infty e^{-g^2} g^{2k+3} \phi_{ij}^{(l)} \, dg, \qquad (A1)$$

where $m_{red} \equiv m_i m_j / (m_i + m_j)$ is the reduced mass and $g \equiv |\mathbf{v}_i - \mathbf{v}_j|/v_{ij}$ is a dimensionless velocity normalized to the thermal velocity $v_{ij} = \sqrt{2k_B T/m_{red}}$. $\phi_{ij}^{(l)}$ are the collision cross sections for a given velocity:

$$\phi_{ij}^{(l)} = 2\pi \int_0^\infty (1 - \cos^l \chi_{ij}) b \, db, \qquad (A2)$$

with the integration over the impact parameter b.

In Eq. (A2) χ_{ij} is the scattering angle,

$$\chi_{ij} = \pi - 2 \int_{r_{ij}^{min}}^\infty \frac{b \, dr}{r^2 \left[1 - \frac{b^2}{r^2} - \frac{V_{ij}(r)}{g^2 k_B T}\right]^{1/2}}. \qquad (A3)$$

Here $V_{ij}(r)$ is the interaction potential between the particle of type i and j, and r_{ij}^{min} is the distance of the closest approach between the repulsive particles, which is the root of the following equation:

$$1 - \frac{b^2}{\left(r_{ij}^{min}\right)^2} - \frac{V_{ij}\left(r_{ij}^{min}\right)}{g^2 k_B T} = 0. \qquad (A4)$$

For a Coulombic interaction between ions with charges Z_i^* and Z_j^*, whether the charges are screened or not, there is a natural scale for the cross-sectional area given by $\phi_0 \equiv \pi \left(Z_i^* Z_j^* e^2\right)^2 / \left(8\pi\epsilon_0 k_B T\right)^2$. Using ϕ_0 to make the integral in Eq. (A1) dimensionless, the collision integrals can be written as [3, 61]:

$$\Omega_{ij}^{(lk)} = \sqrt{\frac{\pi}{m_{red}}} \frac{\left(Z_i^* Z_j^* e^2\right)^2}{\left(8\pi\epsilon_0 k_B T\right)^{3/2}} \mathcal{F}_{ij}^{(lk)}, \qquad (A5)$$

where

$$\mathcal{F}_{ij}^{(lk)} \equiv \frac{1}{2\phi_0} \int_0^\infty dg \, e^{-g^2} g^{2k+3} \phi_{ij}^{(l)}, \qquad (A6)$$

is a generalized Coulomb logarithm. As shown in the detailed work of Baalrud and Daligault [61] in the weak coupling limit for unscreened Coulomb potential, these generalized Coulomb logarithms are related to the Landau-Spitzer $\ln \Lambda$ by the following:

$$\mathcal{F}_{ij}^{(lk)} \sim l(k-1)! \ln \Lambda_{ij}. \qquad (A7)$$

The Coulomb logarithm is given by:

$$\ln \Lambda_{ij} \equiv \ln \left(m_{red} v_{ij}^2 \frac{4\pi\epsilon_0 \lambda_{D,i}}{Z_i^* Z_j^* e^2} \right) \qquad (A8)$$

where $\lambda_{D,i} = \sqrt{(\epsilon_0 k_B T)/(n\langle (Z^*)^2 \rangle e^2)}$ is the screening due to ions. More generally, to include non-integer k in Eq. (A7), the factorial $(k-1)!$ can be replaced by its analytic continuation, the gamma function $\Gamma(k) \equiv \int_0^\infty s^{k-1} e^{-s} ds$. This is a specific case of the more general one corresponding to a central repulsive potential of the form $V_{ij}(r) \sim c_{ij}/r^\nu$. In this case it can be shown (cf. Eq. (10.3,10) in Ref. [6]) that:

$$\Omega_{ij}^{(lk)} = \frac{1}{2}\sqrt{\frac{\pi}{m_{red}}} \frac{c_{ij}^{2/\nu}}{(2k_B T)^{\frac{4-\nu}{2\nu}}} \Gamma\left(k+2-\frac{2}{\nu}\right) \phi_{ij}^{(l)}(\nu),$$
$$(A9)$$

where $\phi_{ij}^{(l)}(\nu)$ is related to the generalized logarithm for Coulombic potentials for which $c_{ij} \sim Z_i^* Z_j^* e^2/(4\pi\epsilon_0)$.

Appendix B: Viscosity of Mixtures in Terms of Burgers Resistant Coefficients

In the Burgers [59] formalism for the kinetic theories for gases, transport coefficients are expressed in terms of resistant coefficients which are inversely proportional to diffusivity:

$$\mathcal{K}_{ij} = \mathcal{K}_{ji} \equiv X_i X_j n \frac{k_B T}{[D_{ij}]_1} = \frac{16}{3} \frac{m_i m_j}{m_i + m_j} n_i n_j \Omega_{ij}^{(11)}.$$
$$(B1)$$

Burgers' collision ratios for Coulombic potentials are given by:

$$z_{ij} = 1 - \frac{2\Omega_{ij}^{(12)}}{5\Omega_{ij}^{(11)}}, \qquad (B2)$$

$$z'_{ij} = \frac{5}{2} + \frac{\left(\Omega_{ij}^{(13)} - 5\Omega_{ij}^{(12)}\right)}{\Omega_{ij}^{(11)}}, \qquad (B3)$$

$$z''_{ij} = \frac{\Omega_{ij}^{(22)}}{\Omega_{ij}^{(11)}}, \qquad (B4)$$

$$z'''_{ij} = \frac{\Omega_{ij}^{(23)}}{\Omega_{ij}^{(11)}}. \qquad (B5)$$

In the first Enskog approach the viscosity for a binary mixture in terms of Burgers coefficient is given by [59]:

$$\eta = \frac{\eta_i + \eta_j + \frac{2\eta_i \eta_j}{E}\left(\alpha_{ij} + \alpha_{ji} - \frac{2 z''_{ij}}{5} + \frac{4}{3}\right)}{1 + \frac{2\eta_i \eta_j}{E}\left(\frac{\alpha_{ij}}{\eta_i} + \frac{\alpha_{ji}}{\eta_j} + \frac{4 z''_{ij}}{15E}\frac{(m_i + m_j)^2}{m_i m_j}\right)}, \qquad (B6)$$

where $i \neq j$ (i and j denoting the two different ion species) and α_{ij} is given by Eq. (30). In the above

$\eta_i \equiv [\eta_i]_1$ is the fluid viscosity of species i given in the first Enskog approach by Eq. (25) with the mixture screening λ (31). Also,

$$E = \frac{2k_B T}{3} \frac{(m_i + m_j) n_i n_j}{\mathcal{K}_{ij}} \qquad (B7)$$

which is the same as in Eq. (28). By using definitions of z''_{ij} in Eq. (B4) and of A in Eq. (29) it follows that Eq. (B6) simplifies to Eq. (27).

We now briefly consider the viscosity of arbitrary multicomponent plasmas. Here i and j range over all species, including $i = j$. In terms of the interspecies viscous collision frequencies

$$\nu_{ij} = z''_{ij} \mathcal{K}_{ij}/m_i n_i = \frac{16}{3} \frac{n_j m_j}{m_i + m_j} \Omega_{ij}^{(22)}, \qquad (B8)$$

the full multicomponent system of viscosity equations has the form

$$\frac{5}{3} n_i k_B T = \eta_{(i)} \sum_j \nu_{ij} +$$
$$+ \sum_j \frac{m_i m_j}{m_i + m_j} \left(\frac{\eta_{(i)}\nu_{ij}}{m_j} - \frac{\eta_{(j)}\nu_{ji}}{m_i} \right) \left(\frac{10}{3 z''_{ij}} - 1 \right) \qquad (B9)$$

This system of equations is solved for the unknown partial viscosities $\eta_{(i)}$, in order to calculate the viscosity of the mixture as $\eta = \sum_i \eta_{(i)}$. Burgers proposed an approximation that avoids the matrix inversion needed to solve (B9). As a first approximation to the full system in (B9) Burgers assumed that the net contribution from the rightmost sum is negligible, which gives:

$$\eta \approx \frac{5}{3} \sum_i n_i k_B T \left\{ \sum_j \nu_{ij} \right\}^{-1}. \qquad (B10)$$

This approximation is exact when $z''_{ij} = 10/3$ and/or the total species collision frequency $\sum_j \nu_{ij}$ is the same for all species i; the latter follows from summing Eq. (B9) over i. In more general circumstances, this approximation is usually accurate to a few percent; and, because it does not involve a matrix inversion, it is a cost-effective model to employ in hydrodynamic codes. In this study, its accuracy was found to be better than 0.2%. Note that the approximation in Eq. (B10), through ν_{ij} terms, only involves viscous collision terms proportional to $\Omega_{ij}^{(22)}$, whereas the full expression in Eq. (B9) also involves diffusive (species transfer) collision terms proportional to $\Omega_{ij}^{(11)}$. For the conditions studied here in D-Ar mixtures with $X_{Ar} > 0.1$, we find $(\nu_{ArAr} \approx \nu_{DAr}) \gg (\nu_{ArD} \approx \nu_{DD})$, such that $\eta \approx (5k_B T/3)(n_{Ar}/\nu_{ArAr} + n_D/\nu_{DAr})$, which depends heavily on interspecies collisions. In the binary case, Eq. (B6) can be recovered from (B9) by making the substitutions $\nu_{ii} = 5n_i k_B T/3\eta_i$ and $\nu_{ij} = 10 n_i k_B T \tilde{\alpha}_{ji}/3E$ for $i \neq j$, where $\tilde{\alpha}_{ji} =$
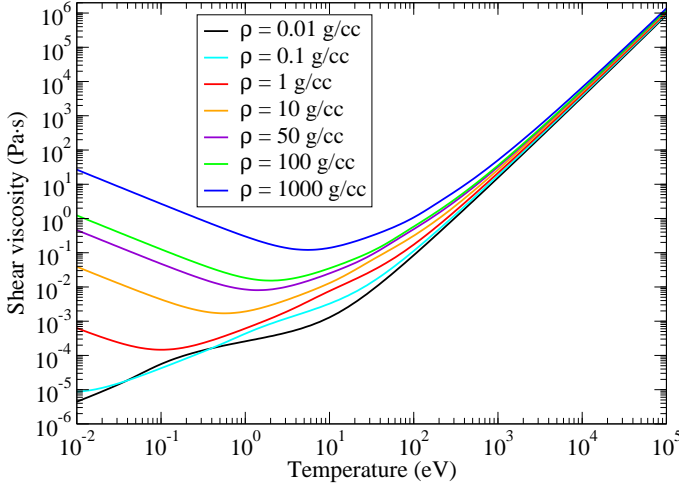
FIG. 9. (Color online) A plot of the shear viscosity of deuterium as determined from the eYVM over a range of temperatures at the densities indicated in the legend.

$(z''_{ij}/5)(n_j/n_i)(m_i + m_j)/m_i$. The approximate viscosity for a binary mixture from Eq. (B10) is

$$\eta \approx \frac{\eta_i + \eta_j + 2\eta_i\eta_j(\tilde{\alpha}_{ij} + \tilde{\alpha}_{ji})/E}{(1 + 2\eta_i\tilde{\alpha}_{ji}/E)((1 + 2\eta_j\tilde{\alpha}_{ij}/E)} \tag{B11}$$

for $i \neq j$.

Appendix C: Extended Yukawa Viscosity Model for Pure Plasmas

Murillo has developed a model for the viscosity of single-species Yukawa systems [19], motivated by an interest in predicting the viscosity of liquid metals and warm dense matter. It is tempting to apply the model to more weakly coupled systems, but it does not provide a good description. In the limit of high temperature and low density, the predicted viscosity goes like the square-root of density times the temperature.

The linear dependence on temperature is consistent with the results of kinetic theory such as the Chapman-Cowling formula if the scattering cross section is independent of temperature, which works for some gases but not others. The dependence on the square-root of density is not consistent with kinetic theory. To attain an improved high-temperature, low-density limit, an extension to the Yukawa Viscosity Model was proposed in Ref. [67]. The only modification is that Eq. (40) is replaced by

$$\eta_0 = \sqrt{\frac{(m\,Z^*)^2\,e^2 n}{\varepsilon_0}} \left(1 + C_1 \frac{1}{\Gamma^3 \mathcal{A}_2^2}\right)^{1/2} \rho\,a^2 \exp\left(-0.2\kappa^{1.62}\right) \tag{C1}$$

We will call this model the extended Yukawa Viscosity Model (eYVM). $\mathcal{A}_2$ is given by

$$\mathcal{A}_2 = 2\left[\log(1 + \tilde{x}_d^2) - \frac{\tilde{x}_d^2}{1 + \tilde{x}_d^2}\right] \tag{C2}$$

$$= \begin{cases} \tilde{x}_d^4 + \cdots & \tilde{x}_d \ll 1 \\ 2\left[\log(\tilde{x}_d^2) - 1\right] & \tilde{x}_d \gg 1 \end{cases} \tag{C3}$$

$$\tilde{x}_d^2 = 16\left(1 + \frac{1}{3\Gamma^3}\right) \tag{C4}$$

Note that were it not for the "1+" in the definition of $\tilde{x}_d$, $\mathcal{A}_2$ and $\mathcal{F}^{(22)}$ would be equal. For Coulomb interaction $\mathcal{F}^{(22)}$ is as follows:

$$\mathcal{F}^{(22)} = 2\left[\log(1 + x_d^2) - \frac{x_d^2}{1 + x_d^2}\right], \tag{C5}$$

$$x_d^2 = \frac{16(k_B T)^2 \lambda_d^2}{(Z^*)^4 (e^2 4\pi\epsilon_0)^2} \tag{C6}$$

$$\lambda_d^2 = \frac{\epsilon_0 k_B T}{n(Z^* e)^2}. \tag{C7}$$

Figure 9 shows the eYVM over a range of temperatures at the densities $\rho = 0.01, 0.1, 1, 10, 100$, and 1000 g/cc. Overall, the model matches the YVM at strong coupling and the Chapman-Cowling model at weak coupling, interpolating between the two at intermediate couplings. There is an anomaly associated with the transition that is evident at low densities. Since the Chapman-Cowling model does not account for screening in the way Paquette-based kinetic models do, the agreement of this model with the MD results is not as good as the hybrid KMD model described in Section V D.

[1] G. Michaud, The Astrophysical Journal **160**, 641 (1970).
[2] G. Fontaine and G. Michaud, The Astrophysical Journal **231**, 826 (1979).
[3] C. Paquette, C. Pelletier, G. Fontaine, and G. Michaud, The Astrophysical Journal Supplement Series **61**, 177 (1986).
[4] H. Ohta and S. Hamaguchi, Physics of Plasmas **7**, 4506 (2000).
[5] J. Lindl, Phys. Plasmas **2**, 3933 (1995).
[6] S. Chapman and T. Cowling, *The Mathematical Theory of Non-uniform Gases: An Account of the Kinetic Theory of Viscosity, Thermal Conduction and Diffusion in Gases*, Cambridge Mathematical Library (Cambridge University Press, 1939).
[7] L. Spitzer, *Physics of Fully Ionized Gases*, Interscience tracts on physics and astronomy (Interscience Publishers, 1962).
[8] J. Daligault, Phys. Rev. Lett. **96**, 065003 (2006).
[9] T. Haxhimali, R. E. Rudd, W. H. Cabot, and F. R. Graziani, Phys. Rev. E **90**, 023104 (2014).
[10] T. Haxhimali and R. E. Rudd, in *Frontiers and Challenges in Warm Dense Matter*, Lecture Notes in Com-

putational Science and Engineering, Vol. 96, edited by F. Graziani, M. P. Desjarlais, R. Redmer, and S. B. Trickey (Springer International Publishing, 2014) pp. 235–263.

[11] C. R. Weber, D. S. Clark, A. W. Cook, L. E. Busby, and H. F. Robey, Phys. Rev. E **89**, 053106 (2014).

[12] B. M. Haines, E. L. Vold, K. Molvig, C. Aldrich, and R. Rauenzahn, Physics of Plasmas **21**, 092306 (2014).

[13] V. Nosenko and J. Goree, Phys. Rev. Lett. **93**, 155004 (2004).

[14] S. J. Putterman, *Superfluid Hydrodynamics*, New York, American Elsevier Publishing Co., Inc. (North-Holland Series in Low Temperature Physics. Volume 3) (Amsterdam, North-Holland Publishing Co., 1974).

[15] L. Landau and E. Lifshitz, *Fluid Mechanics* (Pergamon Press. London, 1963).

[16] J.-F. Dufrêche and J. Clérouin, J. Phys. IV France **10**, 303 (2000).

[17] T. Saigo and S. Hamaguchi, Physics of Plasmas **9**, 1210 (2002).

[18] J. P. Mithen, J. Daligault, and G. Gregori, Contributions to Plasma Physics **52**, 58 (2012).

[19] M. S. Murillo, High Energy Density Physics **4**, 49 (2008).

[20] R. E. Rudd, W. H. Cabot, K. J. Caspersen, J. A. Greenough, D. F. Richards, F. H. Streitz, and P. L. Miller, Phys. Rev. E **85**, 031202 (2012).

[21] J. Daligault, K. O. Rasmussen, and S. D. Baalrud, Phys. Rev. E **90**, 033105 (2014).

[22] K. Y. Sanbonmatsu and M. S. Murillo, Phys. Rev. Lett. **86**, 1215 (2001).

[23] Z. Donkó and P. Hartmann, Phys. Rev. E **78**, 026408 (2008).

[24] S. Bastea, Phys. Rev. E **71**, 056405 (2005).

[25] G. Salin and J.-M. Caillol, Physics of Plasmas **10**, 1220 (2003).

[26] Z. Donkó, J. Goree, and P. Hartmann, Phys. Rev. E **81**, 056404 (2010).

[27] S. Baalrud, K. Ø. Rasmussen, and J. Daligault, Contributions to Plasma Physics **55**, 209 (2015).

[28] G. Salin and D. Gilles, Journal of Physics A: Mathematical and General **39**, 4517 (2006).

[29] N. W. Ashcroft and N. D. Mermin, *Solid State Physics*, Science: Physics (Saunders College, 1976).

[30] B. Firey and N. W. Ashcroft, Phys. Rev. A **15**, 2072 (1977).

[31] Throughout this article we write the formulas in SI units.

[32] H. D. Whitley, D. M. Sanchez, S. Hamel, A. A. Correa, and L. X. Benedict, Contributions to Plasma Physics **55**, 390 (2015).

[33] K. Wünsch, J. Vorberger, and D. O. Gericke, Phys. Rev. E **79**, 010201 (2009).

[34] D. Gilles, F. Lambert, J. Clérouin, and G. Salin, High Energy Density Physics **3**, 95 (2007).

[35] D. Léger and C. Deutsch, Phys. Rev. A **37**, 4916 (1988).

[36] D. Léger and C. Deutsch, Phys. Rev. A **37**, 4930 (1988).

[37] W. Hubbard and H. DeWitt, The Astrophysical Journal **290**, 388 (1985).

[38] S. Ichimaru, *Statistical Plasma Physics: Condensed plasmas*, Frontiers in physics (Westview Press, 2004).

[39] M. S. Murillo, Phys. Rev. E **81**, 036403 (2010).

[40] P. Debye and E. Hückel, Phys. Z **24**, 185 (1923).

[41] T. Ott, M. Bonitz, L. G. Stanton, and M. S. Murillo, Physics of Plasmas **21**, 113704 (2014).

[42] E. E. Salpeter, Australian. Journal of Physics **7**, 373 (1954).

[43] R. P. Feynman, N. Metropolis, and E. Teller, Phys. Rev. **75**, 1561 (1949).

[44] F. R. Graziani, J. D. Bauer, and M. S. Murillo, Phys. Rev. E **90**, 033104 (2014).

[45] J. P. Hansen and I. R. McDonald, *Theory of Simple Liquids* (Elsevier Science, 2006).

[46] G. Kagan and X.-Z. Tang, Phys. Plasma **19**, 082709 (2012).

[47] J. D. Huba, *NRL PLASMA FORMULARY* (Naval Research Laboratory, Washington, DC, 2013) pp. 1–71.

[48] J. D. Kress, J. S. Cohen, D. A. Horner, F. Lambert, and L. A. Collins, Phys. Rev. E **82**, 036404 (2010).

[49] All MD simulations made use of the LAMMPS code described by S. J. Plimpton, J. Comput. Phys. 117, 1 (1995); http://lammps.sandia.gov.

[50] S. Nosé, J. Chem. Phys. **81**, 511 (1984).

[51] W. G. Hoover, Phys. Rev. A **31**, 1695 (1985).

[52] D. Frenkel and B. Smit, *Understanding Molecular Simulation: From Algorithms to Applications*, Computational science (Elsevier Science, 2001).

[53] A. Markmann, F. Graziani, and V. S. Batista, Journal of Chemical Theory and Computation **8**, 24 (2012), http://pubs.acs.org/doi/pdf/10.1021/ct200452h.

[54] R. Zwanzig, Annual Review of Physical Chemistry **16**, 67 (1965).

[55] S. Ichimaru, *Basic Principles of Plasma Physics: A Statistical Approach*, A lecture note and reprint series (W. A. Benjamin, 1973).

[56] J. G. Clérouin, M. H. Cherfi, and G. Zérah, Europhysics Letters **42**, 37 (1998).

[57] L. D. Landau and L. P. Pitaevskii, *Physical Kinetics* (Pergamon Press. London, 1981).

[58] S. I. Braginskii, Rev. Plasma Phys. **1**, 205 (1965).

[59] J. M. Burgers, *Flow Equations for Composite Gases*, Applied mathematics and mechanics (Academic Press, 1969).

[60] S. D. Baalrud and J. Daligault, Phys. Rev. Lett. **110**, 235001 (2013).

[61] S. D. Baalrud and J. Daligault, Physics of Plasmas **21**, 055707 (2014).

[62] A. Lenard, Annals of Physics **10**, 390 (1960).

[63] R. Balescu, Physics of Fluids **3**, 52 (1960).

[64] The adiabaticity here is different from the one used to describe the static screening of the ions from the electrons. While the latter is a consequence of the Born-Oppenheimer approach due to the extensive mass difference, the former is a byproduct of the Green-Kubo approach where we wait long enough so that high frequency components are canceled out.

[65] S. Tanaka and S. Ichimaru, Phys. Rev. A **34**, 4163 (1986).

[66] S. Hamaguchi, R. T. Farouki, and H. E. Dubin, J. Chem. Phys. **105**, 7641 (1996).

[67] R. E. Rudd, LLNL report number LLNL-MI-661976 (2012).